

Chapter 13

Titanium Armor with Gradient Structure: Advanced Technology for Fabrication



S. V. Prikhodko, O. M. Ivasishin, P. E. Markovsky, D. G. Savvakín,
and O. O. Stasiuk

Abstract Developing advanced cost-effective manufacturing technology and production of high-strength titanium-based armor materials is extremely important for the protection of military vehicles and personnel. Titanium alloys are high-strength and lightweight structural materials that can be thermally hardened to the level similar to steels but at much higher compared to steels weight efficiency. Armor plates fabricated using a novel approach, Blended Elemental Powder Metallurgy (BEPM), demonstrate superior antiballistic performance compared to the currently used titanium-based armor materials and can be fabricated at lower cost.

13.1 Introduction

The anti-ballistic protection of land systems, mobility and protection of the fighting vehicles and military personnel is vital in success of defense and anti-terrorist operations. Traditional material for armor is rolled homogeneous or high strength steel [1, 2]. Use of steel armor, however, can increase the overall weight of the fighting vehicle on 15–20%, which change the vehicle mobility, maneuverability, fuel efficiency and requires stronger breaks and more powerful engines [3]. The Army is in search of lightweight substitute for steel armor. Due to the high specific strength of titanium, materials on its base are contemplated as a viable alternative in low-weight armor production [3, 4]. However, when the armor parts are fabricated using traditional cast and wrought technology the feasibility of implementation

S. V. Prikhodko (✉)

Department of Materials Science and Engineering, University of California Los Angeles,
Los Angeles, CA, USA

e-mail: sergey@seas.ucla.edu

O. M. Ivasishin · P. E. Markovsky · D. G. Savvakín · O. O. Stasiuk

G.V. Kurdyumov Institute for Metal Physics, National Academy of Science of Ukraine, Kyiv,
Ukraine

© Springer Nature B.V. 2020

C. Palestini (ed.), *Advanced Technologies for Security Applications*, NATO Science
for Peace and Security Series B: Physics and Biophysics,

https://doi.org/10.1007/978-94-024-2021-0_13

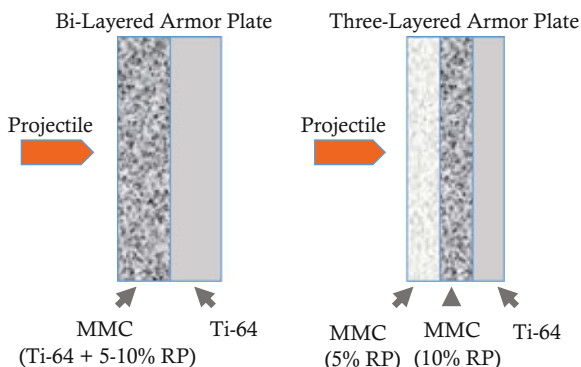
is questionable due to the high cost of the armor parts. In this regard the use of blended elemental powder metallurgy (BEPM) instead of ingot metallurgy of Ti offers an effective cost reduction due to its ability to produce near-net shape parts, while the waste is considerably reduced [5]. Additionally, the price of BEPM fabricated components can be reduced through the use of low-cost hydrogenated titanium powder instead of conventionally used in powder metallurgy (PM) high-cost titanium metal powder [6]. When the sintering is conducted under the vacuum hydrogen can be removed from the final structure, so such approach combines the sintering and dehydrogenation in one processing stage and it has found to be practical in a lot of applications. It was also shown that temporary presence of hydrogen in compact during sintering can have beneficial effect on the final structure since it reduces impurities (including oxygen & chlorine) as well as facilitate the densification of the compact [6]. One of the key benefit of BEPM is that such fabrication can easily facilitate reinforcement of Ti-alloys with hard and light particles, for instance of TiC and TiB making metal matrix composites (MMC) with enhanced elastic moduli without compromising the material's low-weight so desirable for armor. Reinforcement of the alloy with hard particles, however, most likely lowers the value of toughness and plasticity of material. Yet, for durable armor, simultaneous high hardness and high plasticity are not essential through the entire structure: armor parts require high hardness and strength at the surface, whereas their core rather necessitates high toughness and ductility [7]. Such combination of mechanical properties can be achieved on layered structures that combine two and more layers of different materials with different chemical composition and/or microstructure within each individual layer. The objective of this study was development of cost-efficient technology for fabrication of low-weight and exceptional anti-ballistic properties multilayered structures (ML) made using BEPM of Ti alloy and composites on its base with TiB and TiC.

13.2 Experimental Procedure

13.2.1 *Conceptual Design of Multi-layered Plates for Anti-ballistic Application*

Combinations of high strength and ductility can be attained in part for anti-ballistic applications by creation of layered structure, which combines at least two materials with different properties. In manufacturing of armor, it is common to use a layered structures made of a front-facing layer, whose purpose is to blunt and abrade the incoming projectile and a back-facing supporting layer absorbing energy by deformation [7]. In our armor design (Fig. 13.1) we choose to combine the layers of Ti-6Al-4V (wt.%) alloy (Ti-64), which provide sufficient ductility, along with metal matrix composites (MMC) on a Ti-64 base reinforced with TiC or TiB particles to increase hardness. Layers with higher concentrations of reinforcement particles

Fig. 13.1 Design concept of bi- and three-layered armor



have greater hardness. These high hardness layers build the front of the armor part, to enhance wear resistance and to deform and stop projectile upon ballistic impact. The Ti-64 alloy layer with higher ductility and toughness forms the backside of the plate to prevent crack propagation and plate destruction. For multi-layered (ML) structure with more than two layers, we considered different arrangements: (i) with having the hardest layer in the middle of the plate to prevent extensive spallation of this most brittle layer and (ii) in the front of the plate to maximize the abrasion of the projectile.

13.2.2 Fabrication of the Layered Structures Using BEPM

ML structures of Ti-64 alloy and its MMC with 5% and 10% (vol.) of TiC and TiB were fabricated using BEPM of hydrogenated Ti. PM processing utilizing TiH_2 is recognized as low-cost fabrication used in military, aerospace and other critical applications [6]. Four different powder sets of TiH_2 (3.5% H, wt.) with particles sizes (<40, <100, 80–100, 100–125 μm) was used to determine the effect of the base powder size on shrinkage behavior and sintering characteristics of compacts. TiH_2 powder was blended with corresponding amounts of a master alloy powder, 60% Al-40%V (wt.), with particles size <63 μm to form the required Ti-64 composition. To form the MMC layers the required amounts of reinforcement particles powders were added and mixed before the pressing stage. The size of TiC powder particles was <30 μm . In order to obtain TiB inclusions as a part of composite, we used TiB_2 powder particles <20 μm size expected to chemically transform during the sintering via the following reaction: $\text{TiB}_2 + \text{Ti} = 2\text{TiB}$. For the ML structures forming, the blends for each layer were prepared separately and added to the die before pressing. The die pressing (DP) and sintering technique were used to fabricate the samples. Plates, with the dimension 90 × 90 × 18 mm were pressed at 150 MPa; bars 60 × 10 × 10 mm and cylinders 10 mm diameters, 10–12 mm height were pressed at 150 and 640 MPa. Plates were suitable for ballistic test and bars and

cylinders for mechanical tests and structure characterization. Single layer materials were fabricated to test the properties of individual layers. Sintering of all preform samples was conducted in a vacuum furnace (1250 °C, 4 h) followed by slow furnace cooling. Different post-sintering thermomechanical treatments were also conducted.

13.2.3 Structural Characterization of Materials

Structures of materials were characterized using light optical microscopy (LOM), scanning electron microscopy (SEM), electron backscattered diffraction (EBSD), transmission electron microscopy (TEM), x-ray diffractometry (XRD) and x-ray microscopy. Mechanical properties of materials have been evaluated using hardness, microhardness, tensile and 3-point flexural tests. Tensile tests were done on an INSTRON 3376 machine. Following standard protocol, ASTM E8M-04, 3 specimens were tested for individual material, each sample was having the gauge length 40 mm and diameter 4 mm. Three-point flexural tests on the bar samples of sintered bi-layered structures were performed on an INSTRON 8802 following ASTM E290-14 standard. Each value on flexural tests was an average of at least 3 samples tested. The deformation energy was measured based on engineering stress-strain curves obtained on tensile test. Ballistic test was performed in the NATO certified laboratory at Ivan Chernyakhovsky National University of Defense (Ukraine). Seven different bullet types were tested with the bullet weight varied 3.4–10.4 g; speed: 310–930 m/s; kinetic energy 340–3800 J. More details on samples fabrication and characterization protocols used in this project are discussed elsewhere [8, 9].

13.3 Results and Discussion

13.3.1 Structure Characterization of Layered Materials and Some Problems of BEPM Fabrication

Our microscopy results obtained on smaller size layered samples show the grain size of the alloys is generally below 100 μm and for the composite layers is commonly smaller. We observe high structures' compaction and integration between the layers (Fig. 13.2). Details on structures evaluation are reported elsewhere [10, 11]. All layered samples of large dimension (plates) suitable for the ballistic test demonstrate significant linear shrinkage after the sintering. That was result of dehydrogenation of TiH_2 and particles' sintering. Plates with TiC composite, however, were successfully

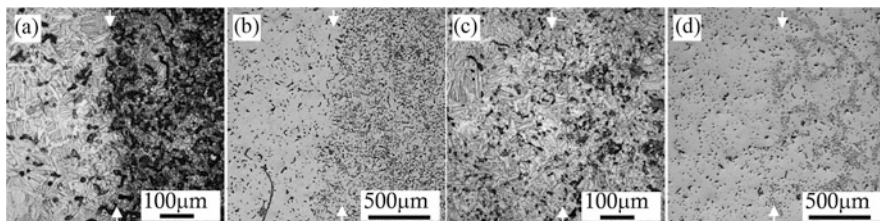


Fig. 13.2 Light optical (a, c) and SEM (b, d) micrographs of bi-layered structures fabricated using BEPM with compression at 640 MPa followed by sintering (1250 °C, 4 h). All images show the structure close to the interface (marked with arrows) between the layers of Ti-64 alloy (left) and MMC on its base (right). The MMC in (a) and (b) 10% TiB; the one in (c) and (d) has 5% of TiC

made using DP protocol owing to very close values of shrinkage of the alloy and TiC composites layers. Shrinkage values measured on plates were 15.7%, 15.5% and 15.1% for Ti-64, Ti-64 + 5%TiC and Ti-64 + 10%TiC layers correspondingly. Insignificant shrinkage mismatch of individual layers didn't cause cracking or distortion of the plates due to the minor interface stress which most likely was compensated by variation in porosity of adjacent layers [9, 11]. Sintering of ML plates with TiB composite was quite different. Those plates demonstrate very different shrinkage values of individual layers: 13.5%, 11% and 8.5% for Ti-64, Ti-64 + 5%TiB and Ti-64 + 10%TiB correspondingly. Shrinkage mismatch builds up the interfacial stress between the layers during the sintering and causes plates bending, delamination and cracking. The difference in shrinkage behavior of layered plates with TiC and TiB was explained using results on dilatometry study of individual powder compacts during continuous heating [9]. It was noted that TiC has very high melting point (3140 °C) and doesn't undergo changes during the sintering. Whereas TiB is a result of in-situ chemical reaction involving diffusion of reacting elements. Due to the large difference in mutual diffusion mobility of boron and titanium it creates the Kirkendall's porosity effect [10]. The increased porosity of TiB composites causes swelling of corresponding layers creating shrinkage mismatch with the alloy.

To minimize the shrinkage mismatch of individual layers during the sintering of ML structures with TiB several experimental parameters were tested. Our assessment on combined effect of the powder size and the powder hydrogen content shows that acceptable (less than 1%) shrinkage mismatches can be achieved at 150 MPa with proper selection of the TiH_2 powder size used. The ML plates suitable for the ballistic test were fabricated using optimized parameters. All details on structure characterization, observed shrinkage mismatch of layered structures during BEPM fabrication and mismatch minimization are reported elsewhere [9].

13.3.2 Mechanical Properties of Layered Structures and Anti-ballistic Performance

Some properties of studied materials are shown in the Table 13.1. Residual porosity of individual layers is strongly affected by the presence and type of reinforcement particles. Ti-64 alloy demonstrates the lowest porosity, which depends on size of TiH₂ powder used for fabrication of ML structures. Porosity of TiC composite is some higher and porosity of TiB composite is the highest. Vickers hardness and tensile properties are pre-determined by the combined effect of residual porosity and the fraction of reinforcement particles. An increasing amount of strengthening particles causes the expected drop in elongation, while the anticipated increase in strength is not observed due to greater porosity and premature fracturing. We observe some increase in Vickers hardness of MMCs. However, the yield stress and ultimate tensile stress values of composites are substantially lower to those values of Ti-64 alloy sintered using optimized parameters (powder size, hydrogen content, compaction pressure) (#7), shown here for comparison.

Our results on 3-point flexure test demonstrated substantial increase in both, the flexure stress and the flexure strain of bi-layered samples compared to a single-layer composite samples as well as the uniform Ti-64 alloy [13]. It was shown that single layer samples of MMC have shown inferior flexure characteristics compared to Ti-64 sample without reinforcement particles. However, when uniform Ti-64 alloy compared to the best bi-layered samples values we see close to 20% improvement of the flexure stress with no loss in the strain value, how it was measured at the same strain rate (10^{-1} s^{-1}) on bi-layered sample with 10% TiC MMC. These results suggest higher deformation energy of bi-layered vs. uniform structures. It is important to note that the order of the layers is essential in the test: the MMC layer must be on the top, where the concentrated load is applied and Ti-64 alloy is at the bottom. When the bar is flipped over the overall flexure performance of the layered structure is far poorer compared to uniform Ti-64 alloy bar. More details are discussed elsewhere [13]. This result implies bi-layered structure of Ti-64//Ti-64 + 10%TiC have potentially better anti-ballistic properties compared to the uniform single-layer Ti-64 and ML structures with TiB prepared using powder approach since it capable absorbing higher energy during deformation. Results on

Table 13.1 Residual porosity, Vickers hardness and tensile properties of individual layers

#	Material	Porosity, %	Hardness, HV	UTS, MPa	Elong., %
1	Ti-64	1.8%	345	1034	7.2
2	Ti-64 + 5TiC	3.8%	333	708	<1
3	Ti-64 + 10TiC	3.6%	373	618	0
4	Ti-64	3.6%	299	969	8.3
5	Ti-64 + 5TiB	4.5%	327	847	0
6	Ti-64 + 10TiB	8%	324	512	0
7 [12]	Ti-64	1.5–1%	320–340	940–1000	10–14

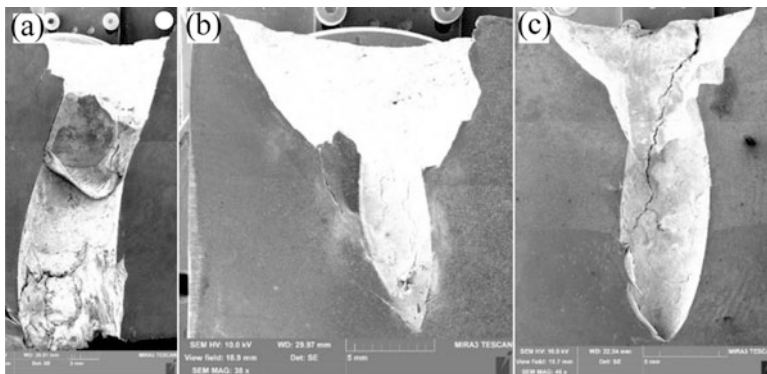


Fig. 13.3 Ballistic test results: (a) Cast Ti-64 alloy; (b) Bi-layered plate of Ti-64 // Ti-64 + 10% TiB; (c) Three-layered plate of Ti-64 // Ti-64 + 10% TiC // Ti-64 + 5%TiC. All plates have about the same thickness 25–27 mm. Test conditions: B32 bullet (Table 13.3), caliber 7.62 × 54 mm, mass 10.4 g, kinetic energy 3500–3800 J. The cast fabricated sample in (a) was annealed at 1100 °C for 1 h and cooled with the furnace producing lamellar microstructure [16]

antiballistic test corroborates with the data on 3-point flexure test. We can see substantially better anti-ballistic performance of the layered structures compared to the cast Ti-64 alloy (Fig. 13.3). Bullets of 7.62 caliber pierced the cast plate all the way through and stuck inside of the layered structures without showing damage on the backside of the tested plate.

13.3.3 *Anti-ballistic Performance of Bi-layered Structures and Potentials of Its Improvement*

Comparing the mechanical characteristics of bi-layered and uniform structures we could expect substantial improvement of anti-ballistic performance of our materials if we have better control over their porosity (Table 13.1). Hardness is one of the most important properties of the front facing layer of the armor as most of the studies suggest and it appears that porosity is undesirable. The data in the Table 13.1 show loss of Vickers hardness with increased porosity, even in the presence of high-moduli particles of TiC and TiB that supposed to contribute to the hardness gain. That is why we attempted hot plastic deformation of sintered ML structures for their more complete densification for the hardness improvement [8]. Ideally such treatment should provide the porosity reduction to about 1–1.5% without imposing uncontrollable grain growth and layers' delamination. Post-sintering hot plastic deformation of different structures was conducted at temperatures not far from the beta-transus of Ti-64 alloy. It was found that the deformation of layered structures using hot rolling was unsuccessful due to significant disparity of the metal flow and degree of accommodated plastic deformation in Ti-64 alloy and adjacent composite

layers. It was established that the hot pressing of the plates was more successful. ML samples with TiC particles were successfully hot pressed at 1100 °C to a total deformation degree of 45%, without breaking the integrity between the layers. At such conditions the deformation degree of Ti-64 alloy layer in the ML structure reached 65% that resulted in reduction of total porosity of this layer to less than 1% and decrease in the pore size. After the hot pressing plates were additionally annealed (850 °C, 2 h) for the stress removal. The deformation behavior of the ML plates used MMCs with TiB was fairly different. The hot pressing was performed at 1100 °C and was stopped at 10% of the total deformation due to the cracks formation started within the MMC layers. More details are reported elsewhere [8]. Thermomechanical processing is still ongoing study, but current results show the potentials on mechanical properties improvement of layered structures after the optimized thermomechanical treatment is applied. We expect further improvement of antiballistic performance of ML. We also consider an alternative approach on layered structures fabrication, which separate layers bonding from the sintering. In such approach optimized treatment could be used separately on each layer followed by the layers' bonding using diffusion bonding (DB), hot isostatic pressing (HIP) or friction welding (FW) etc. Potential predicaments of dissimilar structures bonding are that parameters, which control the process, can affect each structure from the couple differently. Some complications can also arise due to presence of reinforcement particles and other defects. To address the feasibility of ML structures fabrication by joining optimized layers we run some studies on DB, HIP and FW of Ti-64 alloy with MMCs on its base. Results of these studies [14, 15] show successful bonding of Ti-64 alloy and TiB/TiC MMCs on its base via different suggested methods. It validates the prospects of joining of Ti-64 alloy and MMC of this alloy with TiC and TiB to form layered structures and opens possibilities of bonding the structures after each layer processed separately to its optimal performance. Such approach can significantly facilitate the hardness increase of MMC layer since it eases the restrains on the amount of the reinforcement phase. Besides, it takes away the concern on shrinkage mismatch between the alloy and composite during BEPM fabrication. Also it potentially allows welding and bonding the armor of any shape and dimension.

13.3.4 Three-Layered Armor Structures and Its Optimization

Three-layered armor structures have advantage over bi-layered since they allow more flexibility in changing the order and the thickness of the layers with different individual properties in order to better resist on specific ballistic impact [7]. Optimization of three-layered structures was done using flexure test performed on 60 × 10 × 10 mm bars. The goal of this assignment was optimization of three-layered structures in order to minimize the number of ballistic trials. Few variables were in question: (1) type of particles (TiC or TiB); (2) the order of the sheets:

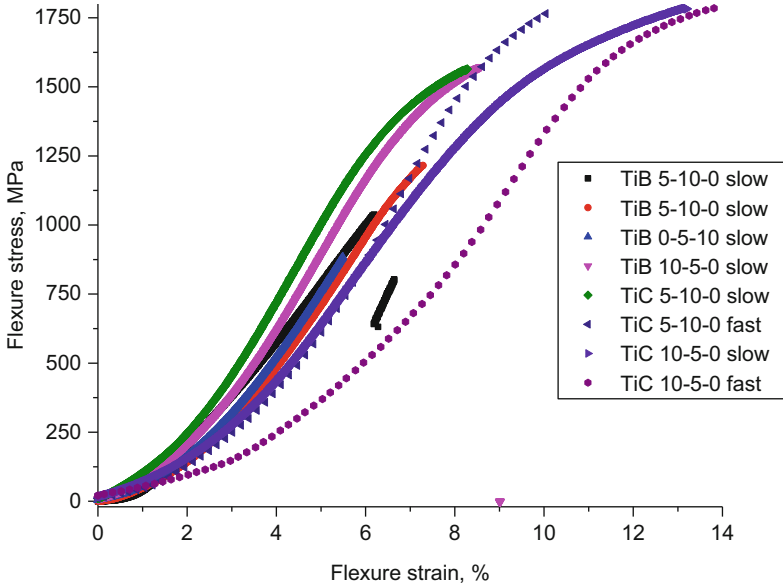


Fig. 13.4 Results on 3-point bend test of three-layered structures. The labels indicate: the type of reinforcement (TiB and TiC); the amount (in vol. %) for the layers at the top-center-bottom of the tested bar (the top layer is where the concentrated load was applied); “fast” and “slow” indicated the strain rate: 10^{-1} s^{-1} and 10^{-3} s^{-1} correspondingly. The thickness of each layer was $\sim 3 \text{ mm}$

the hardest, medium hard and ductile with 10%, 5% and 0% of reinforcement correspondingly; (3) thickness of each layer in triplet; and (4) the strain rate.

Results in Fig. 13.4 show that three-layered structures with TiC perform considerably better compared to the structures with TiB. The best performance of three-layered structures is observed in consequence 10-5-0 with the hardest layer on the top of the tested bar. Among all measured structures with TiB performance was the poorest when the alloy Ti-64 layer was used at the top. We also can see consistently higher flexure stress and strain for the faster strain rate used (dotted lines vs. solid green and purple). Last observation points out on potentially good anti-ballistic properties (ultimate stress increase with increasing the strain rate) of considered structures as existing ballistic theories suggest [7].

We also evaluate the optimum thickness ratio of the sheets in three-layered structures with TiC reinforcement. The consequence of the layers 10-5-0, determined earlier was used. Results of this test (not shown) demonstrate that the highest flexure stress/strain is observed when the used ratio was 2:1:3. It suggests that for the best flexure performance the bottom ductile layer should be about half of the thickness of the entire bar and the top hardest layer (10% of TiC) should be twice thicker than the medium hard (5% of TiC).

Table 13.2 Tested samples in the strain rate evaluation test (in grams)

Composition/sample #	1	2	3	4	5	6
Ti-64 + 10%TiC	10	10	8	8	6	6
Ti-64 + 5%TiC	4	4	4	4	4	4
Ti-64	10	10	12	12	14	14

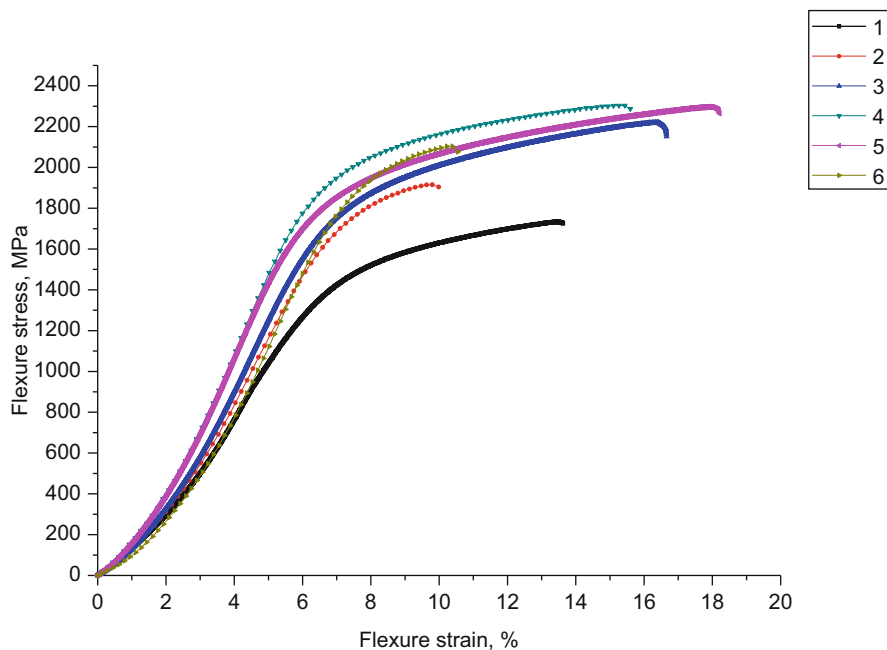


Fig. 13.5 Flexure test results of the three-layered structures in evaluation of the combined effect of the strain rate and the layers' thickness. The number in the label correspond to the sample number in the Table 13.2

Finally, we evaluated the effect of the strain rate on flexure stress-strain behavior of three-layered structures. Even though the optimum ratio 2:1:3 was established in the previous test we wanted to verify it reminds the best when the strain rate is changed. So, basically there were two variables in this test: the strain rate and the layer's thickness ratio. Six tested conditions are listed in the Table 13.2 and results of the experiment are shown in Fig. 13.5. The thickness of each layer in sintered structure was controlled by the mass of the powders used for each layer and it is listed in grams in the label for each curve on the chart. The total mass of entire bar was always the same, 24 g. Samples 1, 3, 5 were tested at 10^{-3} s^{-1} and 2, 4, 6 at 10^{-1} s^{-1} strain rates. Samples #3 and #4 are showing the best combination of strength and ductility and the highest deformation energy at both tested rates. It is also important to note that for those two samples stress is higher at higher strain rate, which points on good anti-ballistic properties. Sample with layer's order 6-4-14 show good result at slow rate (#5), however at fast rate (#6) it performs

poorly. Outcome of this test verifies that the ratio 2:1:3 gives the best antiballistic performance and it was used to fabricate three-layered plates for further ballistic examination.

13.3.5 Ballistic Test of Three-Layered Structures

Examination parameters of selected three-layered plates and results of their ballistic examination are listed in Table 13.3 and some details discussed elsewhere [16].

Seven tested bullets' types are grouped into three classes based on their striking factors. The striking factor of the 1st class bullet (PST, PS, LPS) is the kinetic energy of projectile only (steel bullet, not quenched). The 2nd class (PP) is characterized by two striking factors, kinetic energy and hardened core of the bullet (700 HV). And the 3rd class (BZ, B-32) is characterized by three striking factors, kinetic energy, hardened core and incendiary capability. We determined the threshold Specific Kinetic Energy (SKE) per plate thickness required for piercing three-layered plates by different bullets' classes. Those are summarized as followed:

- when SKE is below 8.88 J/mm^3 the 1st class of bullets is not capable of piercing. When the SKE is higher than 10.77 J/mm^3 the plates are getting consistently pierced;
- for the 2nd class bullet the piercing is taking place at SKE exceeding 8.85 J/mm^3 .
- for the 3rd class the piercing is not happening at SKE of 3.29 J/mm^3 whereas at $5.19\text{--}5.91 \text{ J/mm}^3$ partial piercing (bullets stuck in the plates) can take place.

The SKE calculated in this study was compared to results in two other studies on Ti-64 alloy armor and all three data sets are shown in Fig. 13.6. The armor plates reported in [17] was treated using surface rapid heat treatment (SRHT) that reinforces the surface layer of the armor plate by creating gradient structure. The figure on SKE demonstrates that compared to currently used Ti-64 alloy armor (3) [18] the energy enable the piercing of armor plate is required to be 10-15% higher for Ti-64 alloy armor after its structure is modified by SRHT (2); and it is almost twice (!) higher for the layered structure in this study (1) which incorporate MMC as the front layers.

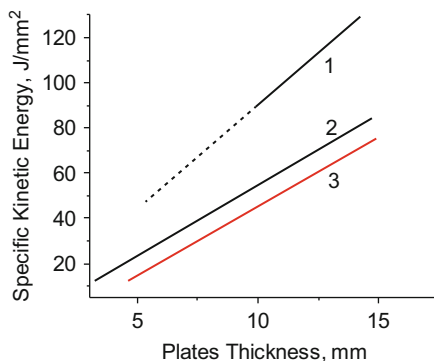
13.4 Conclusions

Relatively big size plates suitable for ballistic test of ML structures of Ti-64 alloy and MMC on its base with 5–10% (vol.) of TiC and TiB were fabricated using BEPM of hydrogenated Ti. It was found that during the sintering of the layered structures the shrinkage levels of the base alloy layer and MMC with TiC are similar, enabling the successful fabrication of multi-layered structures without requiring optimization of the sintering processing parameters for relatively large plates.

Table 13.3 Ballistic examination of three-layered plates

#	Plate composition/state	Bullet type	Bullet mass, g	Bullet speed, m/s	Bullet energy, J	SKE, J/mm ³	Result
1	8/4/12, as-sintered	LPS	9.6	875	3675	11.01	Pierced
2	8/4/12, as-sintered	PP; PS	3.63.5	919908	15201443	8.858.82	PiercedNot pierced
3	6/4/14, as-sintered	LPS	9.6	880	3717	10.77	Pierced
4	6/4/14, as-sintered	PS	3.5	904	1430	8.88	Not pierced
5	8/6/24, as-sintered	LPS; BZ	9.67.4	867753	36082098	5.693.29	Not piercedNot pierced
6	8/6/24, deformed	BZ	7.4	749	2076	5.19	Partially pierced, cracked
7	6/6/28, as-sintered	BZ; B32	7.410.4	751864	20873882	3.285.91	Not piercedPartially pierced
8	6/6/28, deformed	BZ	7.4	750	2081	5.2	Partially pierced

Fig. 13.6 SKE of the 1st class (“soft” core) bullet required to make the armor piercing vs. plate thickness. Chart (1) shows current study results corresponding to the testing condition listed in the Table 13.3, #2 (PS) and #5 (LPS). Chart (2) shows results of previously reported study [17] and (3) of study [18]



The shrinkage level of the Ti-64-based MMC reinforced with TiB is significantly different from that of the alloy layer and requires careful control over sintering parameters. Effective control of shrinkage mismatch between individual layers can be achieved through the careful selection of base powder size and the used amount of hydrogenated Ti powders.

It was found that layered structures fabricated using BEPM protocol with the front facing layer made of MMC and the back facing made of Ti-64 alloy demonstrate superior antiballistic performance compared to the uniform armor plates made using cast and wrought technique of Ti-64 alloy. Superior antiballistic properties of the layered armor structures were explained by their enhanced flexural strength compared to uniform single layer part made of Ti-64 alloy.

The post-sintering thermomechanical treatment, commonly used to increase the densification of the PM products, has major restrictions for the layered structures application. The hot rolling was found to be unsuccessful. The hot pressing at 1100 °C followed by the annealing at 850 °C for 2 h was somewhat promising for porosity reduction of layered structures with TiC MMCs. The effect of hot pressing and annealing on the properties of the layered plates with TiB MMCs was less apparent.

DB and FW can be used for joining sheets of Ti-64 alloy and MMC of this alloy with TiC and TiB to form layered structures. That opens possibilities of bonding the structures after each layer processed separately to its optimal performance. Such approach can significantly improve the properties of individual layer and as a result the entire layered armor. Besides, it takes away the possible concern on shrinkage mismatch between the alloy and composite during the BEPM fabrication of layered components and opens bypass on fabrication of large-sized and complex-shaped structures.

Three-layered armor structures with the layers different by the amount of reinforcement particles were optimized in terms of the layers' thickness and the order. The threshold SKE per plate thickness required for the armor plate to be pierced were determined for three different bullets' classes and found to be superior for ML structures in this study compared to currently used Ti-64 armor.

References

1. Cimpoeru SJ (2016) The mechanical metallurgy of armour steels. Fishermans Bend, Victoria (Australia): Australian Department of Defence; Land Division, Defence Science & Technology Group; Oct. Report No.: DST-Group-TR-3305
2. El-Bitar T, El-Meligy M, El-Shenawy E, Almosilhy A, Dawood N (2017) Thermo-mechanical processing of armor steel plates. *Int J Mater Met Eng* 11(3):214–220
3. Montgomery JS, Wells MGH, Roopchand B, Ogilvy JW (1997) Low-cost titanium armors for combat vehicles. *JOM* 49(5):45–47
4. Pettersson A, Magnusson P, Lundberg P, Nygren M (2005) Titanium–titanium diboride composites as part of a gradient armour material. *Int J Impact Eng* 32:387–399
5. Lutjering G, Williams JC (2007) Titanium. Springer, Berlin/Heidelberg/New York
6. Ivasishin OM, Moxson VS (2014) Low cost titanium hydride powder metallurgy. In: Qian M, Froes FH (eds) Titanium powder metallurgy: past, present and future. Elsevier, Cambridge, MA
7. Crouch IG (2016) The science of armour materials. Elsevier Science & Technology, Cambridge
8. Prikhodko SV, Markovsky PE, Savvakina DG, Stasiuk OO, Ivasishin OM (2018) Thermo-mechanical treatment of titanium based layered structures fabricated by blended elemental powder metallurgy. *Mater Sci Forum* 941:1384–1390
9. Ivasishin OM, Markovsky PE, Savvakina DG, Stasiuk OO, Norouzi Rad M, Prikhodko SV (2019) Multi-layered structures of Ti-6Al-4V alloy and TiC and TiB composites on its base fabricated using blended elemental powder metallurgy. *J Mater Process Technol* 269:172–181
10. Prikhodko SV, Norouzi Rad M, Markovsky PE, Savvakina DG, Julian N, Ivasishin OM (2017) 3D imaging of titanium alloys multi-layered structures (MLS) via X-ray microscopy. *Microsc Microanal* 23(S1):322–323
11. Prikhodko SV, Markovsky PE, Savvakina DG, Stasiuk OO, Norouzi Rad M, Choi C, Ivasishin OM (2018) Characterization of layered structures of Ti-6Al-4V alloy and metal matrix composites on its base. *Microsc Microanal* 24(S1):2218–2219
12. Ivasishin OM, Savvakina DG, Moxson VS, Duz VA, Lavender C (2007) Ti-2007 science and technology: proceedings, 11th world conference on titanium (Kyoto, Japan) (Niinomi M, Akiyama S et al (eds)), vol 1. Japan Institute of Metals, Sendai, pp 757–760
13. Markovsky PE, Savvakina DG, Ivasishin OM, Bondarchuk VI, Prikhodko SV (2019) Mechanical behavior of titanium-based layered structures fabricated using blended elemental powder metallurgy. *J Mater Eng Perform* 59:5772–5792
14. Prikhodko SV (2019) Friction welding of Ti-6Al-4V alloy and metal matrix composites on its base. 5th symposium on linear friction welding, March 20–22, Cambridge
15. Prikhodko SV, Savvakina DG, Markovsky PE, Stasiuk OO, Enzinger N, Deley F, Flipo B, Shirzadi AA, Davies HM, Davies PD, Penny J, Bozhilov KN, Ivasishin OM (2019) Layered structures of Ti-6Al-4V alloy and metal matrix composites on its base joint by diffusion bonding and friction welding. *Microsc Microanal* 25(S2):812–813
16. Ivasishin OM, Markovsky PE, Savvakina DG, Stasiuk OO, Golub VA, Mirmenko VI, Sedov SG, Kurban VA, Antonyuk SL (2019) Microstructure and properties of titanium-based materials promising for antiballistic protection. *Prog Phys Met* 20(2):288–309
17. Ivasishin OM, Akhonor SV, Savvakina DG, Berezos VA, Bondarchuk VI, Stasyuk OO, Markovsky PE (2018) Effect of microstructure, deformation mode and rate on mechanical behaviour of electron-beam melted Ti-6Al-4V and Ti-1.5Al-6.8Mo-4.5Fe alloys. *Prog Phys Met* 19(3):309–334
18. Fanning JC (2005) Military applications for β titanium alloys. *J Mater Eng Perform* 14:686–690